Metal Nanoclusters

Deutsche Ausgabe: DOI: 10.1002/ange.201600267
Internationale Ausgabe: DOI: 10.1002/anie.201600267

Gold Doping of Silver Nanoclusters: A 26-Fold Enhancement in the Luminescence Quantum Yield

Giada Soldan[+], Maha A. Aljuhani[+], Megalamane S. Bootharaju, Lina G. AbdulHalim, Manas R. Parida, Abdul-Hamid Emwas, Omar F. Mohammed, and Osman M. Bakr**

Abstract: *A high quantum yield (QY) of photoluminescence (PL) in nanomaterials is necessary for a wide range of applications. Unfortunately, the weak PL and moderate stability of atomically precise silver nanoclusters (NCs) suppress their utility. Herein, we accomplished a ≥26-fold PL QY enhancement of the $Ag_{29}(BDT)_{12}(TPP)_4$ cluster (BDT: 1,3-benzenedithiol; TPP: triphenylphosphine) by doping with a discrete number of Au atoms, producing $Ag_{29-x}Au_x(BDT)_{12}(TPP)_4$, x = 1–5. The Au-doped clusters exhibit an enhanced stability and an intense red emission around 660 nm. Single-crystal XRD, mass spectrometry, optical, and NMR spectroscopy shed light on the PL enhancement mechanism and the probable locations of the Au dopants within the cluster.*

Noble-metal nanoclusters (NCs), consisting of a precise number of metal atoms and ligands, exhibit unique molecular, optical, and physicochemical properties because of their distinct electronic structures.[1] The typical size of NCs lies in between atoms and plasmonic nanoparticles.[1a,2] Particularly, NCs of gold, silver, and their alloys are being investigated for their potential for light-energy conversion applications,[3] in addition to their catalytic activity,[4] biocompatibility,[5] and tunable emissions in the visible and near-infrared (NIR) regions.[6] The photophysical properties of NCs were found to be influenced by their intrinsic structure, composition, core size, and environment, including solvent and protecting ligand.[1c,7] While luminescent NCs are in high demand, the origin of luminescence is not fully elucidated—with some studies implicating ligand-to-metal charge transfer (LMCT) and/or ligand-to-metal-metal charge transfer (LMMCT).[8] The pivotal roles of the nature of metal atoms and the ligands signify the opportunity to tune the photoluminescence (PL) quantum yield (QY) of NCs for practical applications.[8,9] In this direction, various research groups followed the surface functionalization of NCs with diverse protecting environments, including polymers,[10] thiols,[11] and proteins.[12] Another approach is the alloying or doping of the metal core of a NC with another suitable metal;[13] this method is attractive not only because of the control it affords over the number of alloying atoms, but also because it opens the opportunity to gain fundamental insights into the PL evolution with doping at a single-atom level. For instance, a 200-fold PL QY enhancement was observed when Au_{25} NCs were doped with 13 silver atoms.[14] However, the role of doping on well-characterized Ag NCs—materials that would benefit immensely from enhancing their QY and stability—is still unknown.

Among thoroughly characterized (including X-ray structure) visible-light-emitting Ag NCs, the $Ag_{29}(BDT)_{12}(TPP)_4$ cluster (BDT: 1,3-benzenedithiol; TPP: triphenylphosphine) has moderate stability and weak PL QY (0.9%), where PL is too weak to perceive by the naked eye.[15] In this work, we demonstrate the PL QY enhancement of Ag_{29} NCs by doping with a distinct number of Au atoms while maintaining the Ag_{29} cluster's structural integrity. As a result, the PL QY is increased from 0.9 to 24% (≥26 times) and the fluorescence became visible to the naked eye, which would be useful for colorimetric and sensing applications. In addition, by Au doping, a significant enhancement in the ambient stability of the Ag_{29} cluster is achieved. Single-crystal analysis coupled with mass spectrometry, transient absorption spectroscopy, and nuclear magnetic resonance (NMR) provides insights into the PL enhancement mechanism and probable locations of Au atoms in the doped clusters.

The synthesis of Au-doped Ag_{29} NCs (see the Supporting Information for details) involves the co-reduction of Ag and Au precursors in the presence of BDT and TPP ligands. During the synthesis, the incoming Au precursor concentration was varied from 0–40 mmol% (hereafter, it is denoted by 0–40% Au) to elucidate the effect of doping extent on the optical properties of doped clusters. Figure 1 illustrates the electrospray ionization mass spectrometry (ESI MS) of the Ag_{29} control and the Au-doped Ag_{29} NCs. The ESI MS data was acquired by excluding phosphines (under high dry gas flow during MS measurements)[15] in order to simplify the mass spectral analysis. The Au-doped cluster corresponding to 10% Au exhibits a group of peaks in the three times negatively charged state, the masses of which are larger than $[Ag_{29}(BDT)_{12}]^{3-}$. Each of these groups is separated by m/z 30. A total mass of 30*3 = 90 corresponds to the difference between masses of one Au and one Ag atom. This observation clearly indicates the sequential replacement of Ag atoms of

[*] G. Soldan,[+] M. A. Aljuhani,[+] Dr. M. S. Bootharaju, L. G. AbdulHalim, Dr. M. R. Parida, Prof. O. F. Mohammed, Prof. O. M. Bakr
Division of Physical Sciences and Engineering
Solar and Photovoltaics Engineering Research Center (SPERC)
King Abdullah University of Science and Technology (KAUST)
Thuwal 23955-6900 (Saudi Arabia)
E-mail: omar.abdelsaboor@kaust.edu.sa
osman.bakr@kaust.edu.sa
Dr. A. H. Emwas
Imaging and Characterization Core Lab
King Abdullah University of Science and Technology (KAUST)
Thuwal 23955-6900 (Saudi Arabia)
[+] These authors contributed equally to this work.

Supporting information for this article can be found under: http://dx.doi.org/10.1002/anie.201600267.

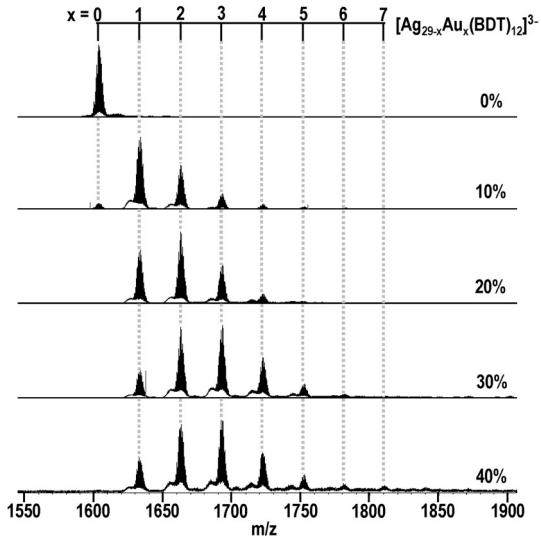

Figure 1. Negative mode ESI MS of $[Ag_{29}(BDT)_{12}]^{3-}$ (0% Au) and its Au-doped NCs $[Ag_{29-x}Au_x(BDT)_{12}]^{3-}$, $x = 1$–7 synthesized by varying the amount (mmol%) of doped Au.

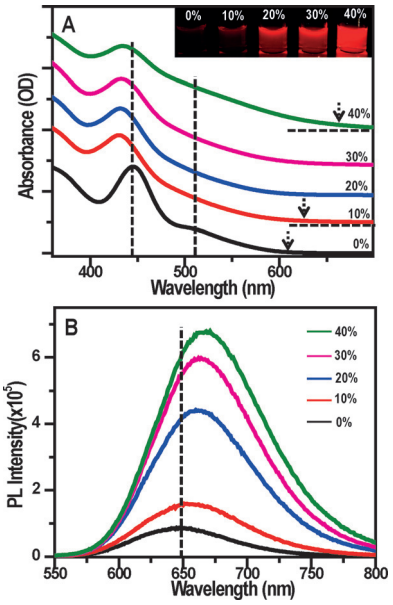

Figure 2. A) UV/Vis and B) PL spectra of Ag_{29} and Au-doped Ag_{29} clusters synthesized using different amounts (mmol%) of Au. Inset: a photograph of Ag_{29} and Au-doped Ag_{29} clusters under a UV lamp (using 365 nm light).

the original Ag_{29} NCs with Au atoms. In the 10% Au sample, at least five Au atoms have been incorporated resulting in $[Ag_{29-x}Au_x(BDT)_{12}]^{3-}$, $x = 1$–5. The successful incorporation of Au atoms into the Ag_{29} NC was further confirmed by the exact match between the simulated and experimental mass spectra (see Figure S1). As the amount of doped Au increased from 10 to 40% during synthesis, the relative intensities corresponding to the alloy clusters that contain more Au atoms are also increased. However, peaks for six and seven Au atom-doped Ag_{29} NCs are also identifiable with comparably negligible intensity.

The optical characterization of $Ag_{29-x}Au_x(BDT)_{12}(TPP)_4$ clusters was carried out using UV/Vis and PL spectroscopy. From the absorption spectra (Figure 2A), it is clear that the incorporation of the Au heteroatoms influences the spectrum by blue-shifting the characteristic Ag_{29} peak at 447 nm (left dotted line) probably because of the modulation in the electronic structure. A similar blue-shift of the UV/Vis peaks was observed while doping Ag_{44}[11a] and Ag_{25}[16] clusters with gold. On the other hand the absorption onset red-shifted (dotted arrows in Figures 2A and S2A) after Au-doping of Ag_{29} NCs. In addition, the shoulder peak at 510 nm (right dotted line) disappeared and the main absorption peak of Ag_{29} at 447 nm broadened with increasing amounts of Au dopant.

Importantly, the PL spectra (Figure 2B) show an increase of fluorescence intensity with an increasing amount (mmol%) of Au. Furthermore, the emission maximum is slightly red-shifted (the shift increased consistently from 658 nm for 10% to 668 nm for 40%) compared to the Ag_{29} control. This red-shift of the PL peak (dotted lines in Figures 2B and S2B) is also consistent with the red-shift in the lower-energy edge of the corresponding UV/Vis absorption data indicating the systemic decrease in the HOMO–LUMO energy gap of the Ag_{29} NCs. A similar PL red-shift was noted for Au_{25} upon doping with Cu.[17] The excitation spectra of Ag_{29} and its 40% Au-doped counterpart substantiate this finding (Figure S2C). The PL QY measurements (see the Supporting Information for details) revealed an increase in the QY from 0.9% for parent Ag_{29} NCs to 19 and 24% for 30 and 40% Au-doped samples, respectively, clearly demonstrating the role of the Au atoms in the QY enhancement. Using large percentages of gold (but not beyond 40 mmol% Au, where $Ag_{29-x}Au_x$ NCs did not form) leads to high QYs.

To understand the electronic origins of the PL enhancement and the effect of Au doping on the excited-state dynamics, we investigated Ag_{29} and its Au-doped analog clusters by femto–nanosecond transient absorption (fs–ns TA) and time-correlated single-photon counting (TCSPC). The experimental setup of fs–ns TA and TCSPC are detailed elsewhere.[18] Upon excitation with a 350 nm laser pulse, a ground-state bleach (GSB) at 445 nm, corresponding to the Ag_{29} absorption, was observed along with the excited-state absorption (ESA) bands at 405 nm and another band with multiple features in the 485–800 nm spectral range (Figure S3A). The TA spectra reveal a notable shift in the GSB position of 435 nm for Au-doped Ag_{29} NCs compared to the undoped one, which is consistent with the ground-state absorption. In addition, a change in the shape of ESA was also observed in the range of 485–800 nm in Au-doped clusters (Figure S3B). The spectral changes in the TA of Au-doped clusters could be attributed to strong perturbation to the electronic structure that occurs when Au atoms are introduced within the Ag_{29} structure.

A fitting of the time profiles of the Ag_{29} NCs representing the GSB gives an exponential decay with a characteristic time constant of 300 ± 35 ns (Figure 3A). This single long-lived component is attributed to a ligand-to-metal charge trans-

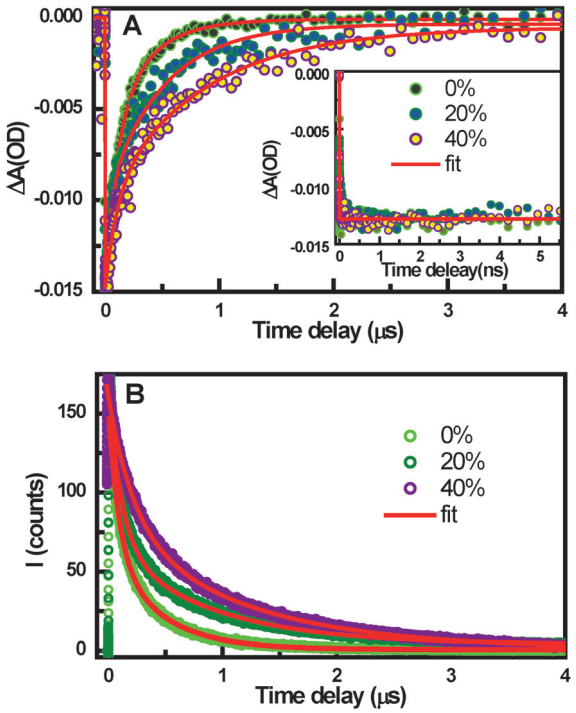

Figure 3. A) Transient kinetic traces corresponding to the GSB from the TA spectra of Ag_{29} and its Au-doped NCs. Inset: kinetics in 0.0–5.5 ns window. B) Kinetics of fluorescence excited-state decay of Ag_{29} and Au-doped clusters at the emission maxima measured by TCSPC. All the solid red lines are fits of the kinetic traces.

fer.[19] The long-lived nature of this excited state is also observed for other silver NCs.[20] The fitting of the time profiles of Au-doped clusters shows two time components as presented in Table S1, unlike pure Ag_{29} NCs, which show just a single dominant lifetime. This implies an involvement of a somewhat different mechanism that causes PL enhancement in Au-doped NCs. As can be seen in Figure 3 A, a clear enhancement in the long lifetime component was observed for 20 and 40% Au-doped samples (612 ± 65 ns and 890 ± 71 ns, respectively). This observation indicates that perturbations to the electronic relaxation and dynamics of the doped clusters are induced by the states formed by the heteroatoms. The enhancement in the PL QY of the clusters depends on the nature of the excited state (S_1), which is affected significantly by increasing the number of doped atoms in the Ag_{29} framework. The S_1 states in the alloy samples result from $Ag_{29-x}Au_x$ clusters with probably varying degrees of metal–ligand charge transfer and/or different degrees of solvation. A high-level theoretical investigation would explain the effect of doping on the structure stability of S_0 and S_1 states which is beyond the scope of this study.

The relaxation dynamics of the pure Ag_{29} control and Au-doped Ag_{29} clusters were also investigated by fs-TA (Figure 3 A inset). Within the 5.5 ns time window, the dynamics of the GSB recovery for Au-doped and undoped cluster shows no change, providing a clear experimental evidence for the absence of any ultrafast dynamical events. To further confirm the excited-state deactivation is radiative, the fluorescence decay was measured using TCSPC (Figure 3 B), which is very similar to the lifetime obtained from TA measurements. This confirms that the presence of two lifetime components in Au-doped clusters is indeed radiative.

Determining the precise positions of Au atoms within the Au-doped Ag_{29} cluster is vital to correlate the clusters structure with the modulated optical properties, including QY enhancement. To resolve the positions of Au atoms, attempts were made to grow single crystals of the Au-doped Ag_{29} clusters (Figure S4). Unfortunately, only species containing a single Au atom crystallized within all samples investigated. As revealed by single-crystal XRD, these species, which represent only a subpopulation of each sample (ranging from 10–40% Au), have one Au atom replacing the central Ag atom of the Ag_{29} NC forming a thermodynamically stable $Ag_{28}Au(BDT)_{12}(TPP)_4$ cluster (Figure 4 B) similar to $Ag_{24}Au(SR)_{18}$.[16] Similar to Ag_{29},[15] no

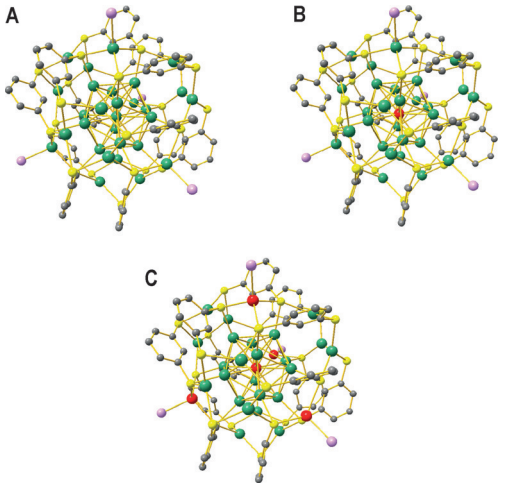

Figure 4. X-ray crystal structures of A) $Ag_{29}(BDT)_{12}(TPP)_4$ and B) $Ag_{28}Au(BDT)_{12}(TPP)_4$. C) Possible locations of Au atoms in $Ag_{29-x}Au_x(BDT)_{12}(TPP)_4$ clusters, $x = 1$–5. Color spheres: green, Ag; red, Au; yellow, S; pink, P; gray, C. For simplicity, H atoms are omitted.[22]

counterions were identified in the $Ag_{28}Au$ crystal structure. However, these clusters (Ag_{29} and $Ag_{28}Au$) possess a superatomic[21] charge of -3 that leads to a close-shell electronic configuration imparting the electronic stability to the cluster. Other compositions, that is $Ag_{29-x}Au_x(BDT)_{12}(TPP)_4$, $x = 2$–5, were uncrystallizable likely because they contain mixtures of Au-doped clusters including all possible isomers that prevented the growth of representative single crystals.

Therefore, to overcome this limitation, we investigated the Au positions using solution-state P NMR analysis, which probes all the population of cluster compositions present in the samples. The P NMR results (Figure 5) of Au-doped clusters displays a systematic shift in P signals with increasing amount (mmol%) of Au in the synthesis. From this observation, we can infer that the Ag atoms that are connected to phosphines were replaced by Au atoms, since the TPP molecules are more labile[15] and weakly bound to Ag than thiolates. There are four phosphines in the Ag_{29} cluster (Figure 4 A) that are bound to four individual Ag atoms.

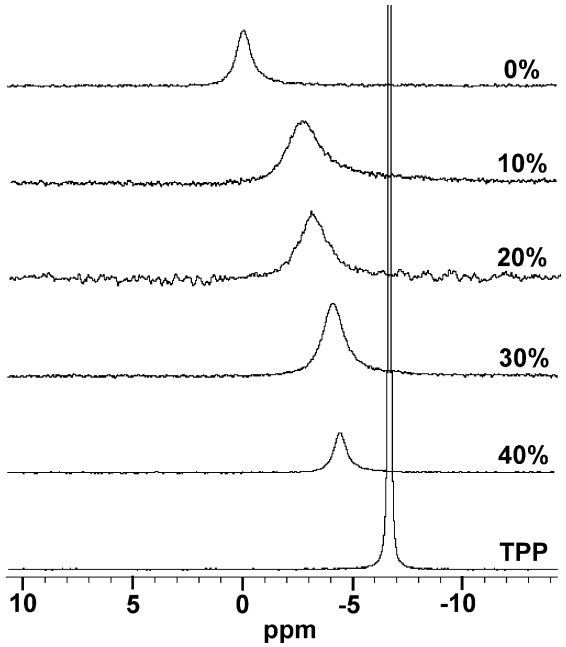

Figure 5. P NMR spectra of pure TPP, $Ag_{29}(BDT)_{12}(TPP)_4$, and $Ag_{29-x}Au_x(BDT)_{12}(TPP)_4$ clusters.

Based on ESI MS (Figure 1) and P NMR results, we propose that the remaining four Au atoms are most likely present at the four phosphine-binding sites (Figure 4C).

In addition to the optical properties, we further investigated the effect of Au doping on the stability of Ag_{29}. The stability of doped and undoped clusters in dimethylformamide (in the dark) was compared (Figure S5). The presence of gold significantly enhanced the stability of the cluster. After two months, 20–40% Au-doped Ag_{29} samples exhibited no signs of decrease in their PL intensity, while pure Ag_{29} and 10% Au-doped samples showed a decrease in the emission intensities that are half of the original values.

In summary, we successfully doped $Ag_{29}(BDT)_{12}(TPP)_4$ NCs with a discrete number of Au atoms to enhance the PL QY by $\geq$26 times by maintaining the structural integrity of the Ag_{29} NCs. Doping of Ag_{29} NCs with Au atoms not only increased the PL intensity but also the ambient stability of the silver clusters. The detailed characterization using single-crystal XRD, optical spectroscopy, mass spectrometry, and NMR spectroscopy provided insights into the PL enhancement mechanism and the possible locations of the Au heteroatoms within the Ag_{29} framework. Our study opens a new path for creating highly luminescent noble-metal nanoclusters, for sensing and colorimetric applications, and also for understanding the origins of the PL in noble-metal alloy nanoparticles at discrete atomic levels.

Acknowledgements

Financial support for this work was provided by KAUST. Part of this work was by Saudi Arabia Basic Industries Corporation (SABIC) grants RGC/3/2470-01 and GIF/5/1830-01.

Keywords: coordination modes · nanoalloys · nanoclusters · photoluminescence · supramolecular chemistry

How to cite: *Angew. Chem. Int. Ed.* **2016**, *55*, 5749–5753
Angew. Chem. **2016**, *128*, 5843–5847

[1] a) R. Jin, *Nanoscale* **2015**, *7*, 1549; b) J. Liu, M. Yu, C. Zhou, S. Yang, X. Ning, J. Zheng, *J. Am. Chem. Soc.* **2013**, *135*, 4978; c) C. P. Joshi, M. S. Bootharaju, O. M. Bakr, *J. Phys. Chem. Lett.* **2015**, *6*, 3023; d) O. M. Bakr, V. Amendola, C. M. Aikens, W. Wenseleers, R. Li, L. Dal Negro, G. C. Schatz, F. Stellacci, *Angew. Chem. Int. Ed.* **2009**, *48*, 5921; *Angew. Chem.* **2009**, *121*, 6035; e) T. Tsukuda, H. Häkkinen, *Protected Metal Clusters: From Fundamentals to Applications*, Elsevier, **2015**.

[2] a) C. P. Joshi, M. S. Bootharaju, M. J. Alhilaly, O. M. Bakr, *J. Am. Chem. Soc.* **2015**, *137*, 11578; b) A. Desireddy, B. E. Conn, J. Guo, B. Yoon, R. N. Barnett, B. M. Monahan, K. Kirschbaum, W. P. Griffith, R. L. Whetten, U. Landman, T. P. Bigioni, *Nature* **2013**, *501*, 399; c) R. S. Dhayal, J. H. Liao, Y. C. Liu, M. H. Chiang, S. Kahlal, J. Y. Saillard, C. W. Liu, *Angew. Chem. Int. Ed.* **2015**, *54*, 3702; *Angew. Chem.* **2015**, *127*, 3773.

[3] Y. S. Chen, H. Choi, P. V. Kamat, *J. Am. Chem. Soc.* **2013**, *135*, 8822.

[4] a) S. Xie, H. Tsunoyama, W. Kurashige, Y. Negishi, T. Tsukuda, *ACS Catal.* **2012**, *2*, 1519; b) S. Wang, S. Jin, S. Yang, S. Chen, Y. Song, J. Zhang, M. Zhu, *Sci. Adv.* **2015**, *1*, e1500441.

[5] X. Le Guével, C. Spies, N. Daum, G. Jung, M. Schneider, *Nano Res.* **2012**, *5*, 379.

[6] S. Gao, D. Chen, Q. Li, J. Ye, H. Jiang, C. Amatore, X. Wang, *Sci. Rep.* **2014**, *4*, 0.

[7] a) C. Zeng, Y. Chen, G. Li, R. Jin, *Chem. Mater.* **2014**, *26*, 2635; b) Y. Yu, Z. Luo, D. M. Chevrier, D. T. Leong, P. Zhang, D.-e. Jiang, J. Xie, *J. Am. Chem. Soc.* **2014**, *136*, 1246; c) A. Eichhöfer, G. Buth, S. Lebedkin, M. Kühn, F. Weigend, *Inorg. Chem.* **2015**, *54*, 9413; d) M. S. Bootharaju, V. M. Burlakov, T. M. Besong, C. P. Joshi, L. G. AbdulHalim, D. Black, R. Whetten, A. Goriely, O. M. Bakr, *Chem. Mater.* **2015**, *27*, 4289; e) E. B. Guidez, V. Mäkinen, H. Häkkinen, C. M. Aikens, *J. Phys. Chem. C* **2012**, *116*, 20617.

[8] Y. Chen, T. Yang, H. Pan, Y. Yuan, L. Chen, M. Liu, K. Zhang, S. Zhang, P. Wu, J. Xu, *J. Am. Chem. Soc.* **2014**, *136*, 1686.

[9] H. Ishida, S. Tobita, Y. Hasegawa, R. Katoh, K. Nozaki, *Coord. Chem. Rev.* **2010**, *254*, 2449.

[10] B. Santiago González, M. J. Rodríguez, C. Blanco, J. Rivas, M. A. López-Quintela, J. M. G. Martinho, *Nano Lett.* **2010**, *10*, 4217.

[11] a) H. Yang, Y. Wang, H. Huang, L. Gell, L. Lehtovaara, S. Malola, H. Häkkinen, N. Zheng, *Nat. Commun.* **2013**, *4*, 0; b) S. Kumar, M. D. Bolan, T. P. Bigioni, *J. Am. Chem. Soc.* **2010**, *132*, 13141.

[12] a) J. S. Mohanty, A. Baksi, H. Lee, T. Pradeep, *RSC Adv.* **2015**, *5*, 48039; b) Z. Luo, K. Zheng, J. Xie, *Chem. Commun.* **2014**, *50*, 5143; c) X. Yuan, N. Goswami, I. Mathews, Y. Yu, J. Xie, *Nano Res.* **2015**, *8*, 1; d) A. Mathew, E. Varghese, S. Choudhury, S. K. Pal, T. Pradeep, *Nanoscale* **2015**, *7*, 14305.

[13] a) X. Le Guével, V. Trouillet, C. Spies, K. Li, T. Laaksonen, D. Auerbach, G. Jung, M. Schneider, *Nanoscale* **2012**, *4*, 7624; b) Y. Negishi, T. Iwai, M. Ide, *Chem. Commun.* **2010**, *46*, 4713.

[14] S. Wang, X. Meng, A. Das, T. Li, Y. Song, T. Cao, X. Zhu, M. Zhu, R. Jin, *Angew. Chem. Int. Ed.* **2014**, *53*, 2376; *Angew. Chem.* **2014**, *126*, 2408.

[15] L. G. AbdulHalim, M. S. Bootharaju, Q. Tang, S. Del Gobbo, R. G. AbdulHalim, M. Eddaoudi, D.-e. Jiang, O. M. Bakr, *J. Am. Chem. Soc.* **2015**, *137*, 11970.

[16] M. S. Bootharaju, C. P. Joshi, M. R. Parida, O. F. Mohammed, O. M. Bakr, *Angew. Chem. Int. Ed.* **2016**, *55*, 922; *Angew. Chem.* **2016**, *128*, 934.

[17] W. Kurashige, K. Munakata, K. Nobusada, Y. Negishi, *Chem. Commun.* **2013**, *49*, 5447.
[18] a) R. Bose, G. H. Ahmed, E. Alarousu, M. R. Parida, A. L. Abdelhady, O. M. Bakr, O. F. Mohammed, *J. Phys. Chem. C* **2015**, *119*, 3439; b) A. A. Alsam, S. M. Aly, A. Usman, M. R. Parida, S. Del Gobbo, E. Alarousu, O. F. Mohammed, *J. Phys. Chem. C* **2015**, *119*, 21896; c) S. M. Aly, G. H. Ahmed, B. S. Shaheen, J. Sun, O. F. Mohammed, *J. Phys. Chem. Lett.* **2015**, *6*, 791.
[19] S. M. Aly, L. G. AbdulHalim, T. M. D. Besong, G. Soldan, O. M. Bakr, O. F. Mohammed, *Nanoscale* **2016**, 8, 5412.
[20] M. Pelton, Y. Tang, O. M. Bakr, F. Stellacci, *J. Am. Chem. Soc.* **2012**, *134*, 11856.
[21] M. Walter, J. Akola, O. Lopez-Acevedo, P. D. Jadzinsky, G. Calero, C. J. Ackerson, R. L. Whetten, H. Grönbeck, H. Häkkinen, *Proc. Natl. Acad. Sci. USA* **2008**, *105*, 9157.
[22] CCDC 1440203 ($Ag_{28}Au$ cluster) contains the supplementary crystallographic data for this paper. These data can be obtained free of charge from The Cambridge Crystallographic Data Centre.

Received: January 10, 2016
Revised: February 23, 2016
Published online: April 6, 2016

